

WIND-TUNNEL MODELLING OF HILL AND VEGETATION

INFLUENCE ON WIND POWER AVAILABILITY

TASK 1: LITERATURE REVIEW

Prepared by

Robert N. Meroney, Ph.D., P.E.*

for

Meteorological Services

U.S. WINDPOWER, INC.

6592 Preston Avenue

Livermore, California 94550

* Professor, Civil Engineering

Director, Fluid Dynamics and Diffusion Laboratory

FLUID MECHANICS AND WIND ENGINEERING PROGRAM

CSU Contract No. 29-8610

CER92-93-RNM-1

October 1992, revised February 1993



WIND-TUNNEL MODELLING OF HILL AND VEGETATION INFLUENCE ON WIND POWER AVAILABILITY

TASK 1: LITERATURE REVIEW

Prepared by

Robert N. Meroney, Ph.D., P.E.*

for

Meteorological Services
U.S. WINDPOWER, INC.
6592 Preston Avenue
Livermore, California 94550

* Professor, Civil Engineering
Director, Fluid Dynamics and Diffusion Laboratory

FLUID MECHANICS AND WIND ENGINEERING PROGRAM

CSU Contract No. 29-8610

CER92-93-RNM-1

October 1992, revised February 1993

Colorado
State
University

EXECUTIVE SUMMARY

A literature review was performed of agricultural meteorology and wind engineering literature to identify the parametric effects of hill shape, vegetation density, and clearing size on hill-top wind speed. Forest meteorology research was examined which considered forest canopy density, tree height, understory structure and tree species effects on wind speed parameters such as displacement height, d ; surface roughness, z_0 ; and surface drag, u_* / u_{ref} . Field and laboratory measurement programs were surveyed which studied the variation of winds downwind of tree stands and the effect of clearings on clearing winds. Numerical and mathematical models were evaluated to determine the state-of-the-art of predictions of combined effects of hill terrain height and vegetation cover on wind fields.

The survey identified several tables and algorithms which may be used to estimate forest canopy displacement height and roughness length. Surface drag data seems to be much less systematic; hence, large variations in magnitude are recorded, and no one algorithm is reliable.

Field and laboratory measurement programs find that the presence or absence of vegetation can produce significant changes in wind speed. Vegetation may also enhance or inhibit the presence of flow separation over hill crests. Limited data taken near wind turbines erected near tree stands confirms that lower turbine productivity occurs at significant distances downwind of vegetation.

Analytic models based on linear-perturbation theories were identified which can predict the combined effects of hill height, hill slope, hill shape and surface roughness variation on hill top wind speeds. These perturbation models have been validated against field and laboratory measurements, and they are found to predict trends correctly, but in some cases may overpredict hill crest wind speeds. Numerical models (FLOWSTAR, MS3DJH/3) based on linear-perturbation methods and Fourier decomposition of complex terrain are available which can predict the joint effects of terrain elevation, thermal stratification, and non-homogeneous surface roughness. These models are constructed to work on small workstations or PC computers. These models are currently limited to stationary situations, "mild" terrain and roughness variations, and mild stratification such that flow separation and blocking do not occur.

Spreadsheet results are provided which estimate the added value of different size clearcut areas over various two-dimensional ridges. Predicted information includes depth of the inner layer of the flow at crest height, wind speeds in the outer and inner region, and fractional speed-up factors. Data is provided for roughness change speed-up, hill induced speed-up, and combined effect of hill slope and roughness variations.

Alternative diagnostic models based on the concept of mass consistency are also available which have been used to examine hill crest flows in the presence of vegetation (NOABL, UICWINDS, NUWINDS, ASL, etc.) Some of these models use ad hoc type modifications to allow for stratification and vegetation effects. These models are also limited to flows which have no separation or blocked regions.

Some authors have also proposed modifications to finite difference or finite element equation sets to account for vegetation drag on wind fields (HOTMAC, CSURAMS). The principle adjustment used is the addition over the vegetation filled portion of the grid of a drag term related to vegetation density. These models have been used to predict winds over meso-scale size regions, are often computer memory and time intensive, and require a fast workstation with considerable memory.

Robert N. Meroney, Professor
Fluid Mechanics and Wind Engineering
Civil Engineering, Colorado State University

ACKNOWLEDGEMENTS

The author wishes to acknowledge the assistance and discussions provided by Dr. Scott Veenhuizen, formerly of United Industries, Inc., Kent, WA; Dr. Michael Sestak, Bureau of Land Management, Fort Collins, CO; Ms. Bernadette Connell, Dr. Evgeny Donev, Dr. William Massman and Dr. Karl Zeller of the Rocky Mountain Forest and Range Experiment Station, Fort Collins, CO; Dr. Tetsuji Yamada, Yamada Science and Art, Inc., Los Alamos, NM; and Dr. Peter Taylor, York University, Canada. The effective and friendly assistance of Mr. Lindsey Weiss of the Colorado State University library staff is also appreciated.

TABLE OF CONTENTS

EXECUTIVE SUMMARY	i
ACKNOWLEDGEMENTS	iii
LIST OF TABLES	vi
LIST OF FIGURES	vii
LIST OF SYMBOLS	xi
I. INTRODUCTION	1
II. WIND FLOW OVER HILLS/COMPLEX TERRAIN	2
2.1 <u>General Wind Speed and Turbulence Characteristics</u>	2
2.2 <u>Field and Laboratory Measurements</u>	9
2.3 <u>Summary</u>	10
III. WIND FLOW OVER VEGETATIVE CANOPIES	17
3.1 <u>Flow Within and Downwind of an Individual Tree</u>	19
3.2 <u>Under-canopy Forest Flow Field</u>	26
3.3 <u>Above-canopy Forest Flow Field</u>	30
3.3.1 <i>Logarithmic velocity profile models</i>	30
3.3.2 <i>Power-law velocity profile models</i>	35
3.4 <u>Wind Flow Near Clearings, Clearcuts, and Forest Edges</u>	38
3.5 <u>Change of Surface Roughness</u>	52
3.5.1 <i>Change of Roughness Models</i>	52
3.5.2 <i>Multiple changes of roughness</i>	55
3.6 <u>Summary</u>	55
IV. VEGETATIVE/SURFACE ROUGHNESS EFFECTS ON FLOW OVER HILLS /MOUNTAINS	57
4.1 <u>Homogeneous Surface Roughness Over Hills/Mountains</u>	57
4.1.1 <i>Field and Laboratory Data</i>	57
4.1.2 <i>Inviscid -Rotational Numerical Model Results</i>	60
4.1.3 <i>Turbulence Model Insights</i>	60
4.1.4 <i>Linear-perturbation Model Insights</i>	60
4.2 <u>Change in Roughness Effects on Flow Over Hills/Mountains</u>	64
4.2.1 <i>Linear-perturbation Model Insights</i>	64
4.2.2 <i>Field and Fluid Model Data</i>	65
4.3 <u>Laboratory Measurements of Vegetation Covered Terrain</u>	65
4.4 <u>Summary</u>	71

V.	ANALYTIC AND NUMERICAL MODELS	72
5.1	<u>Mass-consistent or Objective Analysis Models Applied to Vegetation Covered Terrain</u>	72
5.1.1	<i>NOABL Predictions for Clearcut Effects Over Cape Blanco, Oregon</i>	73
5.1.2	<i>Atmospheric Science Laboratory (ASL) Model Predictions</i>	77
5.1.3	<i>NUATMOS Predictions of Complex Terrain Flows</i>	77
5.2	<u>Linear-perturbation Models Applied to Vegetation Covered Terrain</u>	81
5.2.1	<i>FLOWSTAR Model Predictions</i>	81
5.2.2	<i>MS3DJH and MS-MICRO Model Predictions</i>	81
5.2.3	<i>Mass-consistent and Linear-perturbation Model Comparisons</i>	87
5.3	<u>Primitive Equation Models Applied to Vegetation Covered Terrain</u>	87
5.3.1	<i>HOTMAC Predictions of Forest and Vegetation Effects</i>	87
5.3.2	<i>FITNAH Vegetation Modifications to Predict Deforestation Effects on Drainage Flows and Local Climate</i>	89
5.4	<u>Spread-sheet Predictions of Wind Effects of Clearcutting</u>	91
5.4.1	<i>Linear-perturbation Expressions for Combined Changes in Roughness and Elevation</i>	91
5.4.2	<i>Results of Spreadsheet Calculations</i>	91
5.5	<u>Summary</u>	102
VI.	CONCLUSIONS	103
	APPENDIX: REVIEW AND CLASSIFICATION OF COMPLEX TERRAIN MODELS	105
	REFERENCES	125

LIST OF TABLES

Table 2.2.1	Laboratory Simulations of Flow Over Complex Terrain	12
Table 2.2.1	(Continued)	13
Table 2.2.1	(Continued)	14
Table 2.2.1	(Continued)	15
Table 2.2.1	(Concluded)	16
Table 3.3.1	Table of roughness length data	32
Table 3.4.1	Wake behavior of buildings, trees and shelterbelts (Meroney, 1977)	45
Table 4.1.4	Maximum increase of velocity in potential flow over various two- dimensional hills with low slopes.	61
Table 5.2.1	MS3DJH/3R and finite-difference model predictions for flow over Gaussian hills with roughness modulation. (Walmsley <i>et al.</i> , 1986)	84

LIST OF FIGURES

Figure 2.1.1	Characteristic wind speed and power availability over the crest of a two-dimensional ridge.	3
Figure 2.1.2	Velocity, turbulence, and static pressure profiles over a 1:6 slope triangular hill. (Meroney, et al., 1976)	4
Figure 2.1.3	Velocity, turbulence and static pressure profiles over a 1:4 slope triangular hill. (Meroney, et al. 1976)	5
Figure 2.1.4	Velocity, turbulence, and static pressure profiles over a 1:2 slope triangular hill. (Meroney,et al. 1976)	6
Figure 2.1.5	Velocity speedup between approach flow and crest over different hill shapes. (Meroney et. al. 1978)	7
Figure 2.2.1	Vertical profiles of speedup at the hilltop for two wind directions in wind-tunnel (AES, OXR, NZR) and full-scale (FS) flows (Teunissen <i>et al.</i> , 1987)	11
Figure 3.0.1	Drag coefficients of live and model trees: Dashed line (after Hsi and Nath, 1968); solid circles (after Rayner, 1962) (Meroney, 1968)	18
Figure 3.1.1	Geometry of idealized trees for numerical calculations. (Gross, 1987)	20
Figure 3.1.2	Vertical profiles of u at different point along the symmetry axis. The dotted line shows the undisturbed profile of the inflow boundary. (Gross, 1987)	21
Figure 3.1.3	Vertical profiles of shear stress, σ , at different points along the symmetry axis. The dotted line shows the reference (inflow) value. (Gross, 1987)	22
Figure 3.1.4	Streamlines of the horizontal airflow for 1 m above the ground. The contour of the tree is dotted, the dashed line indicates cases where $u < 0$. (Gross, 1987)	23
Figure 3.1.5	Vertical profiles of u at different points along the symmetry axis (——— ball-tree, - - - cone-tree) (Gross, 1987)	24
Figure 3.1.6	Wind deformation and the wind velocity that may produce that deformation. (Hewson <i>et al.</i> , 1979)	25
Figure 3.2.1	Meteorological wind tunnel at Colorado State University and artificial tree canopy. (Meroney, 1968)	27
Figure 3.2.2a	Velocity profiles in and above model forest canopy (Meroney, 1968)	28
Figure 3.2.2b	Longitudinal turbulent intensity for model forest canopy. (Meroney, 1968)	28
Figure 3.2.3	Under-forest canopy mean velocity profiles for expressions developed by Cowan, 1968; Inoue, 1953, and Cionco, 1965; and Massman, 1987.	29
Figure 3.2.4	Optimal fits of observed wind profile for a Ponderosa pine canopy. Observations are denoted by circles from Raupach and Thom (1981).(Massman, 1987)	29
Figure 3.3.1	Above canopy wind profiles for various average forest canopy heights when $d = 0.63 h$, $z_0 = 0.125 h$, and $u_* = 0.316 u(h)$	34

Figure 3.3.2	Effective roughness for sinusoidal orography. Measurements, finite difference models, and Equation 3.3.4. (Grant and Mason, 1990)	36
Figure 3.3.3	Variation of the power-law index with increasing roughness and corresponding roughness classes for Equations 3.3.8 and 3.3.9. (Baron, 1981)	37
Figure 3.3.4	Variation of the power-law index with increasing height of roughness elements. (Baron, 1981)	39
Figure 3.3.5	Variation of the power-law index with increasing roughness length. (Baron, 1981)	40
Figure 3.4.1	Windflow and vertical profiles of meteorological variables within and above a forest. (Cionco, 1982)	41
Figure 3.4.2	Figure 3.4.1 with smoke plumes deployed. (Cionco, 1982)	41
Figure 3.4.3	Mean velocity profiles within and above the roughness. (Kawatani, 1971)	42
Figure 3.4.4	Shear plate drag for model forest canopy (Meroney, 1968)	43
Figure 3.4.5	Study areas in the High Ridge Evaluation Area, Umatilla National Forest, Oregon. (Fowler, <i>et al.</i> , 1987)	47
Figure 3.4.6	Wind passage at 6 and 20m in watersheds 4 and 1 during two 11 month periods--one before and one after treatment. (Fowler <i>et al.</i> , 1987)	48
Figure 3.4.7	Goodnoe Hills, WA. Radials show directions to towers. Percent reduction in wind speed and increase in turbulence [$\Delta U\%/\Delta u'\%$] (Elliott and Barnard, 1990)	49
Figure 3.4.8	Wind speed ratios (to tower 9) versus tower 9 wind direction. Directions of major groves and wind turbines are indicated (Elliott and Barnard, 1990)	50
Figure 3.4.9	Turbulence intensity ratios (to tower 9) versus tower 9 wind direction. (Elliott and Barnard, 1990)	51
Figure 3.5.1	Wind profile transition height resulting from a change in surface roughness (Park Schwind, 1977, in Meroney, 1977)	53
Figure 3.5.2	Wind profile shapes and wind power profile shapes for various types of flat terrain. (Park and Schwind, 1977)	54
Figure 3.5.3	Internal boundary layer thickness versus normalized distance referenced to larger z_0 . Line is best fit to points. (Hunt and Simpson, 1982)	56
Figure 4.1.1	Effect of surface roughness on wind flow over a sharp-crested ridge. (Wegley, Orgill and Drake, 1978)	58
Figure 4.1.2	Fractional speedup ratio profiles at crest of triangular hills. Field data, Bradley (1978); Laboratory data, Bouwmeester <i>et al.</i> (1978)	59
Figure 4.1.3	Approach flow velocity profiles for numerical inviscid flow calculations. (Bouwmeester <i>et al.</i> , 1978)	62
Figure 4.1.4	Fractional speedup ratios predicted from numerical inviscid flow calculations (Bouwmeester <i>et al.</i> , 1978)	62
Figure 4.1.5	Flow over elliptical obstacles. Heights are scaled by object height. Velocities are scaled by upstream velocity at $z/h = 3$. (Jensen and Petersen, 1978)	63

Figure 4.2.1	Measured fractional speed-up at top of the smooth and rough hills. (Britter <i>et al.</i> , 1981)	66
Figure 4.2.2	Horizontal isotachs over Rakaia Gorge, N.Z. $z_p = 10$ m. (Meroney <i>et al.</i> , 1978)	67
Figure 4.2.3	Horizontal isotachs over Rakaia Gorge, N.Z., $z_p = 50$ m. (Meroney <i>et al.</i> , 1978)	68
Figure 4.2.4	Vertical section G-G isotachs at Rakaia Gorge, N.Z. (Meroney <i>et al.</i> , 1978)	69
Figure 4.2.5	Vertical section F-F isotachs at Rakaia Gorge, N.Z. (Meroney <i>et al.</i> , 1978)	70
Figure 5.1.1	Smoothing scheme for aerodynamic roughness length (Lin <i>et al.</i> , 1985)	74
Figure 5.1.2	Vertical wind profiles over a surface of smoothed surface roughness (Lin <i>et al.</i> , 1985)	75
Figure 5.1.3	Initialization of vertical wind profiles for 3-D wind flow computations. (Lin <i>et al.</i> , 1985)	76
Figure 5.1.4	Typical complex terrain scenario with grass and forest (Δ) vegetation and villages (\square). (Cionco, 1982)	78
Figure 5.1.5	Surface layer windfield solution for Figure 5.1.4. (Cionco, 1982)	78
Figure 5.1.6	Schematic of 3-dimensional coupled wind model (Cionco, 1982)	79
Figure 5.1.7	Cross-section analysis of adjacent grid point wind profiles. (Cionco, 1982)	80
Figure 5.2.2	Crest velocities for sinusoidal hill and $\ln[z_o]$, ———MS3DJH/3R; Finite diff. $m_r = 4$. (Walmsley <i>et al.</i> , 1986)	83
Figure 5.2.1	Sinusoidal hill & $\ln[z_o]$. ——— MS3DJH/3R, finite diff. model, $m_r = 4$; + , $m_r = 100$. (Walmsley <i>et al.</i> 1987)	83
Figure 5.2.4	Crest velocities over rough-crested 2-D Gaussian hill (See Figure 5.2.3 for notation) (Walmsley <i>et al.</i> , 1986)	85
Figure 5.2.3	Rough-crested 2-D Gaussian hill, ($2\beta = 1000$ m, $h = 100$ m, $m_r = 10$) ——— u , --- roughness only fd model; \bigcirc , + roughness only MS3DJH/3R model,	85
Figure 5.2.7	Cresttop velocities for the Coastal Hill and Island experiments. (Walmsley <i>et al.</i> , 1986)	86
Figure 5.2.6	Wind speed at $z = 2$ m for Coastal and Island experiments. Dashed curves are roughness change alone. (Walmsley <i>et al.</i> , 1986)	86
Figure 5.2.8	Mean wind speeds for each of 12 directions computed by WAsP, NOABL*, and MS-MICRO and measured values at Vounaros. (Lalas <i>et al.</i> , 1988)	88
Figure 5.3.1	Distribution of tree canopies. Units are in decimal, <i>i.e.</i> , 3 indicates 0.3, 2 for 0.2, and 0 for no trees. (Yamada and Bunker, 1989)	90
Figure 5.3.2	HOTMAC modeling of horizontal wind vectors at $z = 24$ m at 0200 LST. (Yamada and Bunker, 1989)	90
Figure 5.3.3	Computed wind vectors at 2 m above Finkenbach valley terrain: (a) with canopy, (b) after deforestation. (Gross, 1987)	92

Figure 5.4.1	Linear-perturbation. Inverse-polynomial hill. $h_{\text{hill}} = 100$ m, $L = 1000$ m, $z_{o1} = 3.71$ m, $z_{o2} = 0.1$ m. $U_{10m} = 10$ m/s.	94
Figure 5.4.2	Effects of clearcutting upwind to the hill half-height, $h_{\text{hill}}/L = L$ for various hill slopes. $z_{o1} = 3.71$ m.	95
Figure 5.4.3	Influence on windspeed of clearcutting different distances upwind for a hill slope $h_{\text{hill}}/L = 0.10$. $z_{o1} = 3.71$ m.	96
Figure 5.4.4	Influence on wind speed of clearcutting different distances upwind for a hill slope $h_{\text{hill}}/L = 0.20$. $z_{o1} = 3.71$ m.	97
Figure 5.4.5	Influence on windspeed of clearcutting different distances upwind for a hill slope $h_{\text{hill}}/L = 0.40$. $z_{o1} = 3.71$ m.	98
Figure 5.4.6	Influence on windspeed of clearcutting various distances upwind for hill slope $h_{\text{hill}}/L = 0.10$, $z_{o1} = 1.85$ m.	99
Figure 5.4.7	Influence on windspeed of clearcutting different distances upwind for hill slope $h_{\text{hill}}/L = 0.20$, $z_{o1} = 1.85$ m.	100
Figure 5.4.8	Influence on windspeed of clearcutting different distances upwind for hill slope $h_{\text{hill}}/L = 0.40$, $z_{o1} = 1.85$ m.	101

LIST OF SYMBOLS

<u>Symbol</u>	<u>Description</u>	<u>[Dimension]</u>
A	Silhouette area	[L ²]
C _D	Drag coefficient	
C _f	Skin friction coefficient	
C _p	Surface pressure coefficient	
d	Displacement height	[L]
D	Crown diameter	[L]
h, h _{hill} , H	Hill, mountain, or escarpment height	[L]
h, H	Forest canopy height	[L]
K	Tree crown height	[L]
H	Peak to trough height sinusoidal terrain	[L]
l, l _z , δ ₁	Inner layer depth	[L]
l _{zh}	Inner layer depth for hill effects	[L]
l _{zr}	Inner layer depth for roughness change	[L]
L	Distance from crest to hill half-height	[L]
L	Hill characteristic width	[L]
L _{mo}	Monin-Obukhov stratification scale	[L]
ΔP	Fractional power change	
Ri	Richardson number	
S	Horizontal area occupied by roughness element	[L ²]
ΔS	Fractional speedup factor	

SYMBOLS (Contd.)

<u>Symbol</u>	<u>Description</u>	<u>[Dimension]</u>
ΔT	Fractional turbulent intensity change	
u, U, V	Wind speed	$[LS^{-1}]$
u_h	Wind speed at top of vegetative canopy	$[LS^{-1}]$
u_o	Upwind wind speed	$[LS^{-1}]$
u_{ref}	Reference wind speed	$[LS^{-1}]$
u_*	Surface friction velocity	$[LS^{-1}]$
u_{*1}	" " " due to upwind roughness	$[LS^{-1}]$
u_{*2}	" " " due to downwind roughness	$[LS^{-1}]$
Δu	Perturbation wind speed increment	$[LS^{-1}]$
Δu_{hill}	" " " " " from hill	$[LS^{-1}]$
Δu_{rough}	" " " " " from roughness	$[LS^{-1}]$
x, y, z	Coordinate distances	$[L]$
$z, \Delta z$	Vertical distance above ground	$[L]$
z_o	Surface roughness	$[L]$
z_{o1}	" " " upwind	$[L]$
z_{o2}	" " " downwind	$[L]$
z_o^{eff}	Effective surface roughness from both hills and local roughness	$[L]$
z_m	Matching height	$[L]$
α	Power-law velocity exponent	
β	Deacon's parameter	
κ	von Karman's coefficient	
λ	Wavelength, sinusoidal hills	$[L]$
δ	Boundary layer thickness	$[L]$

I. INTRODUCTION

Wind turbine aerodynamics is concerned with the interaction between atmospheric flows and the turbine's rotor. The wind-turbine rotor operates in the atmospheric surface layer, where wind shear, gustiness, and the local micro-meteorology of terrain shape and vegetation change the operating environment. Since wind turbine performance is critically linked to the availability of wind energy at turbine hub height, preferred sites are those with moderate and persistent winds (20-40 mph).

Hills or ridges are known to cause wind "speed-up" associated with streamline convergence. Convergence will occur in neutrally stratified flows at hill crest; whereas maximum streamline convergence will often occur on the lee of a hill or ridge when the wind flows between the surface and an elevated inversion. Tall vegetation such as woods, wind-breaks, or forests may degrade the wind environment over a hill. Eddies created by a tree canopy can enhance surface mixing reducing near-surface wind speeds, and the eddies themselves may cause gustiness which increases turbine blade loading and fatigue.

Given the simple-minded assumption that wind power is proportional to wind-speed cubed, even a 10% decrease in hub-height winds speed may reduce available wind power by 25%. Thus, knowledge of how vegetation cleared regions over hills may enhance or diminish hill crest velocities would be valuable planning information. Often the key question is how much clear cutting on the site of a proposed wind energy farm is required along the ridge tops and hilltops to maximize wind resources while minimizing environmental impact.

Wind energy specialists have focused frequently on the potential for wind speed amplification found in hilly terrain. Their concerns have led to additional field and laboratory data on the behavior of neutral and stratified flows over both two-dimensional ridges as well as three-dimensional isolated hills, valleys and gorges. Agricultural and forest meteorologists are concerned with "blow-down" in vegetative canopies during wind storms and the air transport of insects, pheromones, insecticides, herbicides, moisture, CO₂, soil, burning debris and smoke. Analytic and numeric models have been created to estimate wind flows above and within such canopies in complex terrain situations.

This review will focus primarily on information related to the operation of wind turbines on hill crests partially or totally covered with forests. Chapter 2 provides a short background about flow amplification over terrain covered with minimal vegetation (*ie.* no flow displacement and small local roughness; $d = 0.0$, $z_0 = 0-0.10$ m). Chapter 3 summarizes what is understood about wind flow over vegetative canopies over essentially horizontal ground surfaces. Chapter 4 considers the joint effects of vegetation and roughness effects over hills/complex terrain. Analytic, physical and numerical models used to characterize such flows are noted in Chapter 5. Conclusions relevant to the problem of wind turbine installation in vegetated hilly terrain are provided in Chapter 6.

II. WIND FLOW OVER HILLS/COMPLEX TERRAIN

The earth's surface is covered with almost imperceptible bulges and depressions on the global scale. The highest mountain barriers only extend above the earth's radius by about one-tenth of one percent from its sea level value. Nevertheless, the presence of hills, mountains and valleys determines a great portion of the weather we live within. Mountains and hills and valleys induce variations in wind speed and turbulence from the mean sufficient to justify location of wind energy devices in complex terrain. Unfortunately, for most of man's weather experience most measurements have been made over flat homogeneous sites. Thus, the understanding of wind flows over complex terrain has become a special area of meteorological consideration. Interest in weather modification, air pollution, and wind energy over the last twenty years has led to extensive additional information about mountain climatology. Today, there are numerous books and monographs specifically focusing on the climate and specifically the winds developed over complex terrain (Blumen, 1990; Frost and Shieh, 1981; Hiester and Pennell, 1981; Hunt and Simpson, 1982; Wegley et al., 1978).

2.1 General Wind Speed and Turbulence Characteristics

Single hills and isolated ridges are known to produce higher wind speeds at a given height over the crest than far upwind during high speed neutrally stratified air flow. The approximate improvement in wind speed should be of the order of h/L , where h is hill height above the surrounding terrain and L is some characteristic horizontal hill width (say the distance from the crest to half-hill height). Thus, a smooth surfaced hill with average approach slopes ($h_{\text{hill}}/(2L)$) of 0.10, 0.2, 0.3, 0.4, or 0.5 should produce fractional speedup [$\Delta S = (u(z) - u_o(z))/u_o(z)$] increases at crest of the order 20%, 40%, 60%, 80% and 100%, respectively, or corresponding order increases in wind power up to 73%, 174%, 309%, 483%, and 700%, respectively (See **Figure 2.1.1**). Speedup does not seem to be as sensitive to hill shape for the same average slope as long as flow separation does not occur (See **Figure 2.1.2**). These values may be reduced by the presence of forests, local undulations, and regions of flow separation. In particular, when hill slopes exceed 0.3 it is likely that flow separation may occur at hill crest decreasing wind speeds and inducing large gustiness. **Figures 2.1.3 through 2.1.4** display wind and turbulence profiles measured over different slope triangular hills in a boundary-layer wind tunnel (Bouwmeester et al., 1978). Fractional speed up is defined as $\Delta S = (u(z) - u_o(z))/u_o(z)$, where $u_o(z)$ is the upstream profile and z is the height above local grade. Typically wind decreases at the foot of the hill then accelerates to hill crest. Over steep hills separation may occur at the hill crest (**Figure 2.1.4**), which decreases crest wind speeds and produces gustiness and excess turbulence downstream.

Figure 2.1.5 displays the effect of 2-dimensional hill shape on fractional wind speedup. Note that hill slope is more significant than hill shape on defining wind profiles as long as the elevation is not so abrupt as to generate separation regions downwind. Three dimensional hills are found to produce lower wind speed increases than similar cross-section ridges.

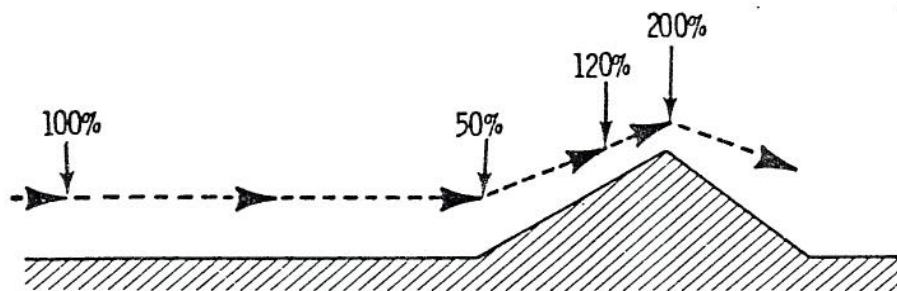


Figure 2.1.1 Characteristic wind speed and power availability over the crest of a two-dimensional ridge.

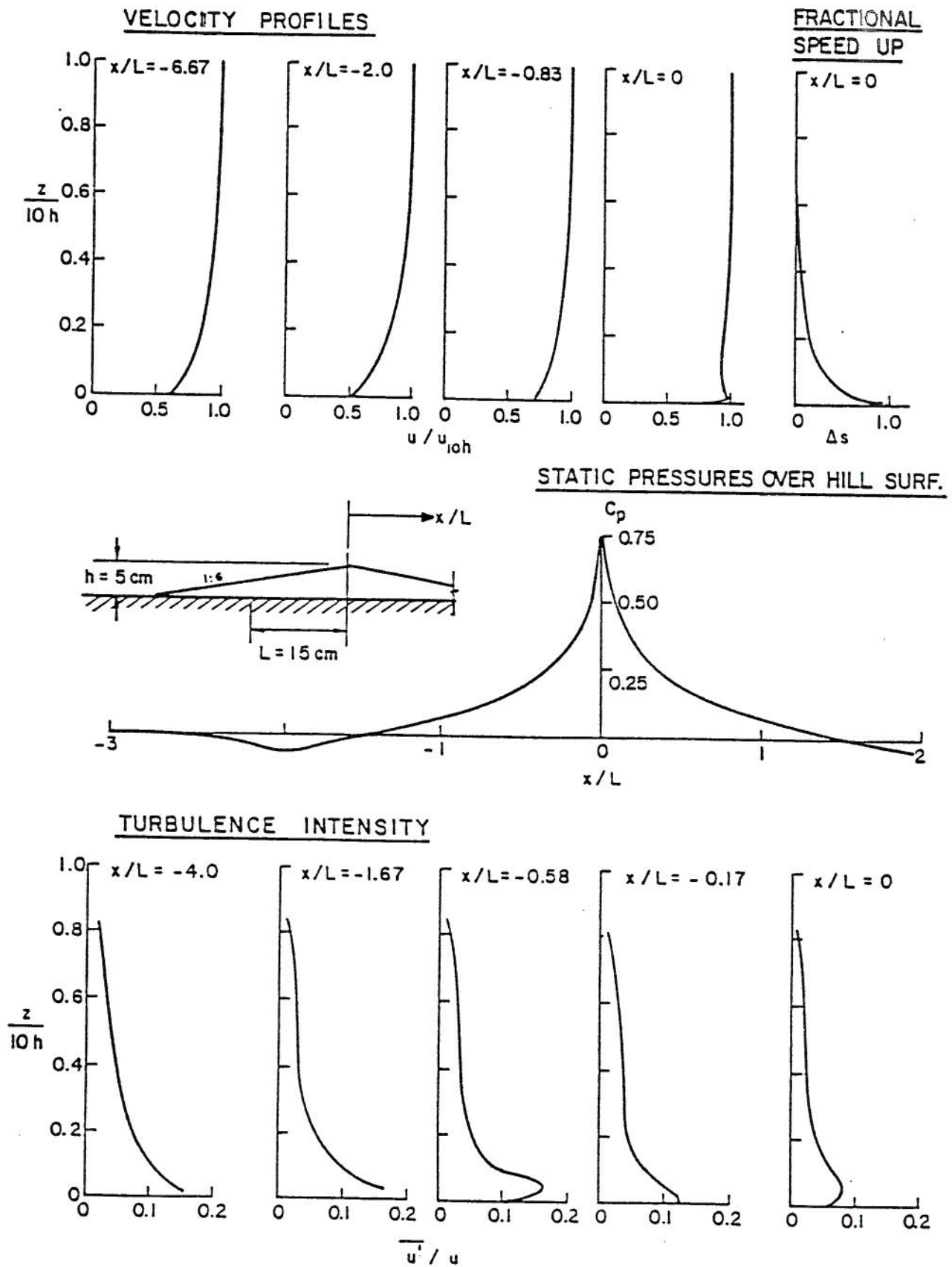


Figure 2.1.2 Velocity, turbulence, and static pressure profiles over a 1:6 slope triangular hill. (Meroney, et al., 1976)

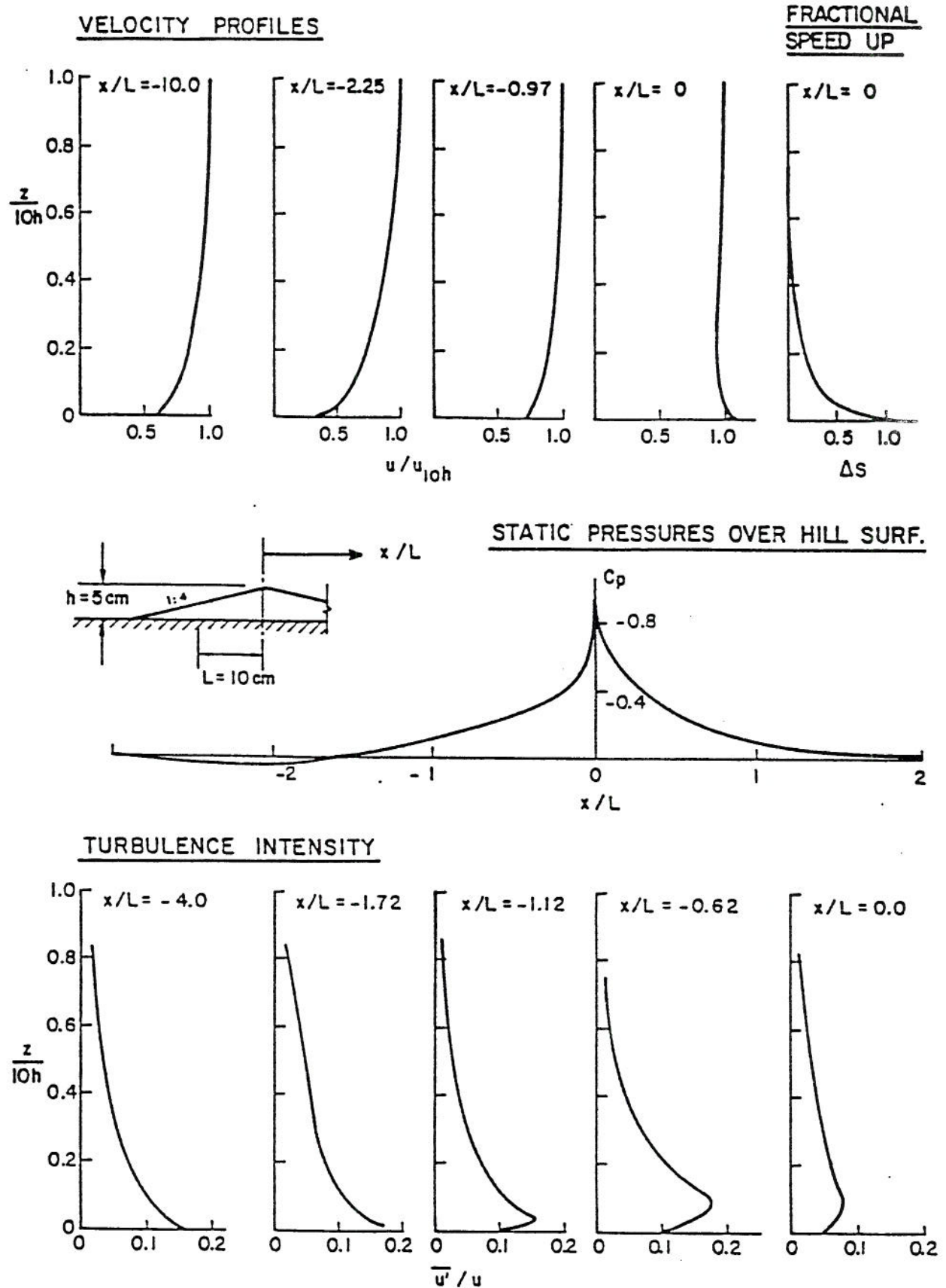
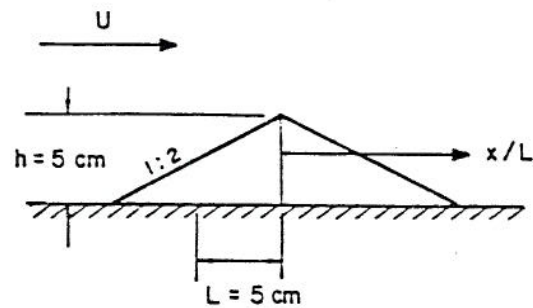
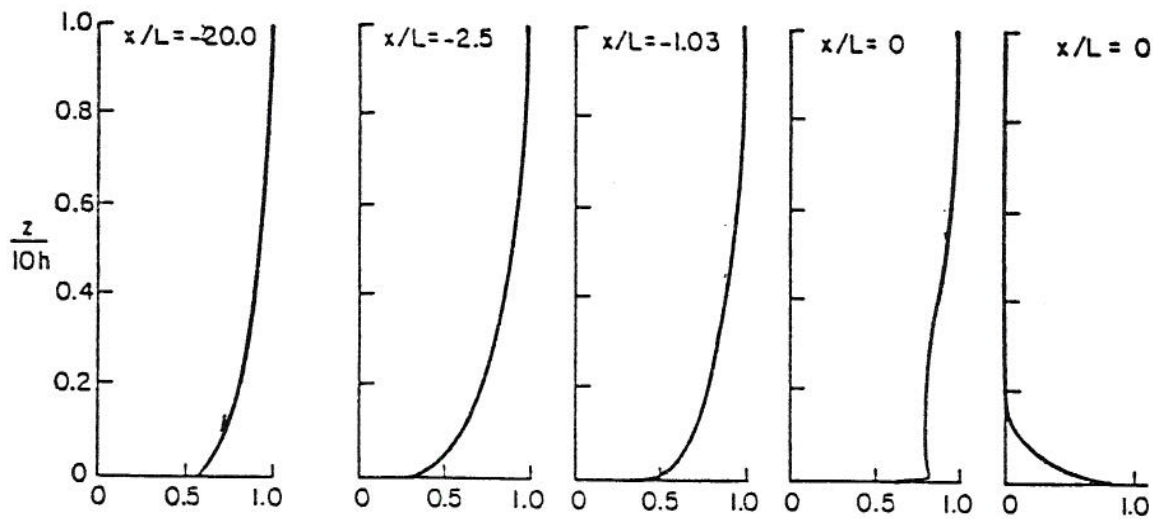


Figure 2.1.3 Velocity, turbulence and static pressure profiles over a 1:4 slope triangular hill. (Meroney, et al. 1976)

VELOCITY PROFILES

FRACTIONAL SPEED UP



STATIC PRESSURES OVER HILL SURFACE

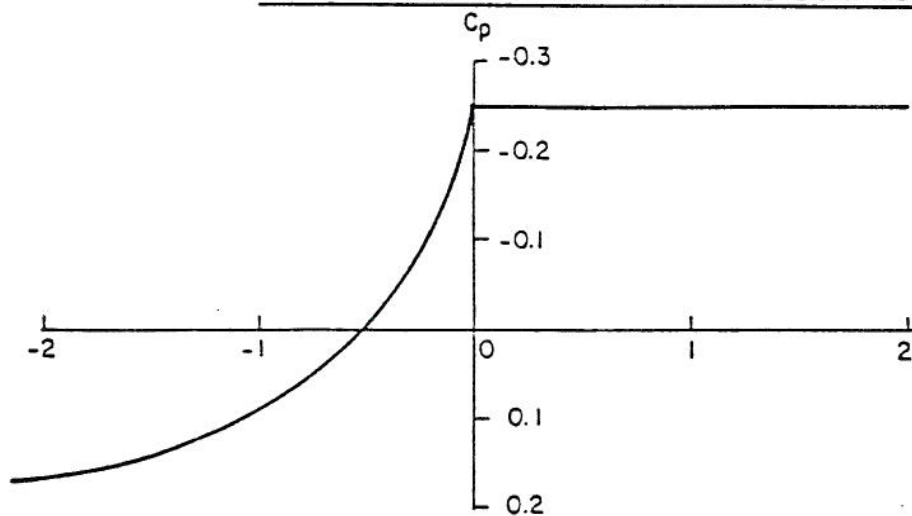


Figure 2.1.4 Velocity, turbulence, and static pressure profiles over a 1:2 slope triangular hill. (Meroney, et al. 1976)

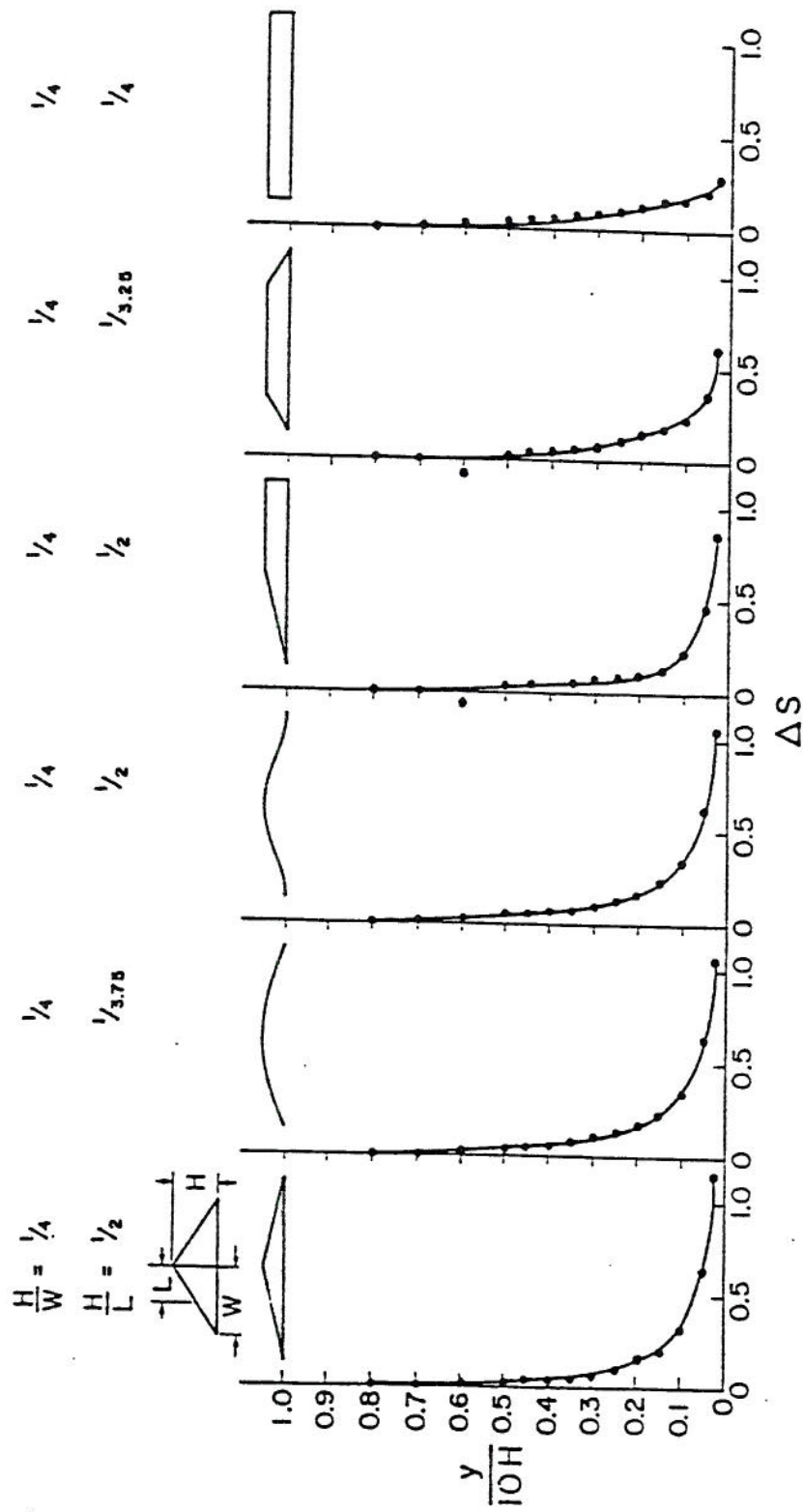


Figure 2.1.5 Velocity speedup between approach flow and crest over different hill shapes.
(Meroney et. al. 1978)

It is more difficult to predict quantitatively the exact wind patterns in complex terrain where multiple hills, mountains and valleys occur over an extensive area. Flow interactions, blocking, and channeling may either enhance or decrease wind speeds. Indeed, at the present state of the meteorological art the serious wind-turbine meteorologist may be limited to field measurements, large meso-scale numerical models, or physical models in such cases.

Thermal stratification will also change the air flow over single hills and mountains substantially. Stable stratification may cause low level winds to move laterally around a hill barrier decreasing crest top winds but enhancing hill side winds, or alternatively an elevated inversion just above hill crest may induce very strong winds on the downslope side of a hill or ridge. Indeed some of the most persistent and attractive wind-energy locations appear to be associated with such downslope conditions. Blumen (1990) has edited a series of articles about such flows in hills, mountains and valleys into a monograph on atmospheric processes over complex terrain. In particular chapter 4 on mountain waves and downslope winds by D.R. Duran, chapter 5 on perturbation solutions to flow over hills by D.J. Carruthers and J.C.R. Hunt, and chapter 7 on physical modeling of flow over hills and mountains by R.N. Meroney are relevant reading for the wind-energy climatologist interested in wind power meteorology in hills and mountains.

Turbulence behavior over hills depends upon upwind fetch, strength of stream line convergence over the crest, and regions of increased shear. For small hills such that surface flows have limited time to come into local equilibrium with the new hill flow conditions the upwind turbulence is primarily advected along streamlines with minor changes; hence changes in wind shear play a small role. On the other hand convergence and divergence of streamtubes may lead to "rapid-distortion" or stretching, twisting, or shortening of turbulent vortex elements. Stretching distortions can lead to enhanced local vorticity and increased turbulence. When the local turbulent velocity is scaled by local mean speed at the hill crest the net effect may be a decrease in turbulent intensity although in absolute terms the turbulent fluctuations are greater. Of course if separation over the crest occurs then elevated regions of increased turbulence downwind will occur.

Hills or mountains with small slope or long upwind fetch conditions permit the near ground flow to move toward local equilibrium with local shear. An inner boundary layer, l_z , grows upward in which these effects are significant. To a first order the depth at crest should be related to $l_z \ln[l_z/z_0] = 2\kappa^2 L$, where z_0 is surface roughness and L is characteristic hill width.¹ For most conditions $l_z = 0.05 L$ when h/L is of order one. In such conditions over

¹ The characteristic hill width, L , may be defined in at least three different ways. It can be total base-width of hill from upstream base to downstream base; it can be the distance from up- or down-wind hill base to hill crest; or it can be the distance from hill crest to the location up- or down-wind where the hill is one-half the total hill height above the base. The half-height width is used for characteristic width throughout this report.

moderate slope hills analytic and numerical methods based on linear-perturbation concepts work quite well (See Section 5.0). To a first order the fractional wind speedup, ΔS , is still found to be proportional to h/L .

2.2 Field and Laboratory Measurements

As a result of environmental and energy concerns there now exists a large number of field data sets related to wind flow fields over hilly and mountainous terrains. Some were performed to answer questions about nuclear power safety, others were concerned with atmospheric transport of power plant plumes, and some were specifically posed to evaluate wind-energy potential over hill crests. Articles in Blumen (1990) refer to experiments of the Dept. of Energy ASCOT test series (Geysers, CA; Brush Creek, CO), the Environmental Protection Agencies CTMDP test series (Cinder Cone Butte, ID; Hog Back Ridge, NM; Tracy Power Plant, NV), and various international measurement efforts like the Askervein hill project (US, NZ, UK, CN). Meroney (1978, 1980) reviews pre-1980 field studies which had laboratory counterpart experiments (eg. Rakaia River Gorge, NZ; Gebbies Pass, NZ; Kahuku Point, Oahu, HA). During the 1980s a number of field studies over relatively smooth isolated hills and ridges were performed specifically to validate wind flow models proposed to predict wind-energy potential (Askervein Hill, Blashaval, Brent Knoll, Great Dun Fell, Nyland Hill, UK; Kettle Hill, CAN). Table 2.2.1 summarizes some details of 69 laboratory studies for 31 cases of which comparable field measurements are available.

Almost all of the isolated hill and ridge studies examined terrain with very small surface roughness (1-3 cm); hence, there are few published data (found during this review) for wind flow over simple terrain shapes incorporating forests, woods, shelterbelts, clearings or clearcut areas. (This is not to say individual meteorological measurements do not exist in clearings and clearcut areas in hills, but no extensive sets of measurements were made in such situations to document terrain wide flow.) One exception was the two-dimensional ridge study performed in Australia by Bradley (1978) (See discussion in Section 4.1).

The ASCOT Brush Creek study involved a 650 m deep valley in western Colorado where the southwest-facing walls were dry, and barren, while the northeast-facing walls were moist and brush covered. The vegetation was found to make a significant difference in diurnal absorption of thermal radiation, and the wind flows which developed in the valley. The ASCOT Geyser area study were performed over tree covered hills and meadow covered valleys. Again inclusion of the vegetation in analytic and numerical models was necessary to reproduce the wind flows observed. Unfortunately, no high wind conditions were observed in either ASCOT study, for the principal program goal was to evaluate the mechanisms of night time and daytime drainage flow in open-ended valleys.

An extensive set of physical model experiments were also performed during the 1980s. The Askervein Hill Project was a collaborative study of boundary-layer flow over low hills (Taylor and Teunissen, 1987). Two field experiments were conducted during fall 1982 and 1983 near and around Askervein, a 116 m high hill on the west coast of the island of South Uist in

the Outer Hebrides of Scotland. Over 50 towers were deployed and instrumented for wind measurements. Most were cup anemometers mounted on simple 10 m posts, but two 50 m, one 30 m, one 16 m, and thirteen 10 m towers were instrumented for three-component turbulence measurements. Subsequently, wind tunnel simulations of the hill were carried out at three different length scales (1 to 800, 1 to 1200, and 1 to 2500) in two wind tunnel facilities (Teunissen et al. 1987). The wind-tunnel results compared well with each other and with full scale data (**Figure 2.2.1**). Changes in mean flow speedup over the physical models were reproduced very well, including those due to small local terrain features that may be physically small at model scale. Relaxation of the aerodynamic roughness criterion ($Re_* = u_* z_0 / \nu > 2.5$) affected the flow only on the lee side of the model hills. Turbulence changes induced by the hill did not depend on the nature of the surface roughness (suggesting the inner boundary length was quite small). An excessively smooth surface reduced the degree and extent of separated flow and resulted in overestimation of hill crest wind speeds. Simulations in two facilities using three models at three different scales showed a gratifying degree of consistency. The only effect of model scale was a predictable increase in difficulty in making measurements very close to the surface as the size of the model decreased. The depth of the turbulent inner layer was similar to the value predicted by Jensen et al. (1984) discussed in Section 3.5.

2.3 Summary

The general behavior of wind flow over simple and complex terrain is qualitatively well understood. Measurements in field or laboratory situations have been made under an amazingly broad range of conditions. Nonetheless, the possible combinations of hill shape, slope, surface roughness, stratification conditions, upwind approach conditions, surrounding terrain undulations, and unsteadiness associated with the diurnal cycle and weather result in few quantitatively reliable estimators for hill crest wind speeds.

Actual measurements of wind flow over vegetation covered terrain which can be used to specify the effect of forest edges, clearings or clearcuts on wind energy siting are minimal. The few studies identified will be discussed in Sections 3.5 and 4.2.

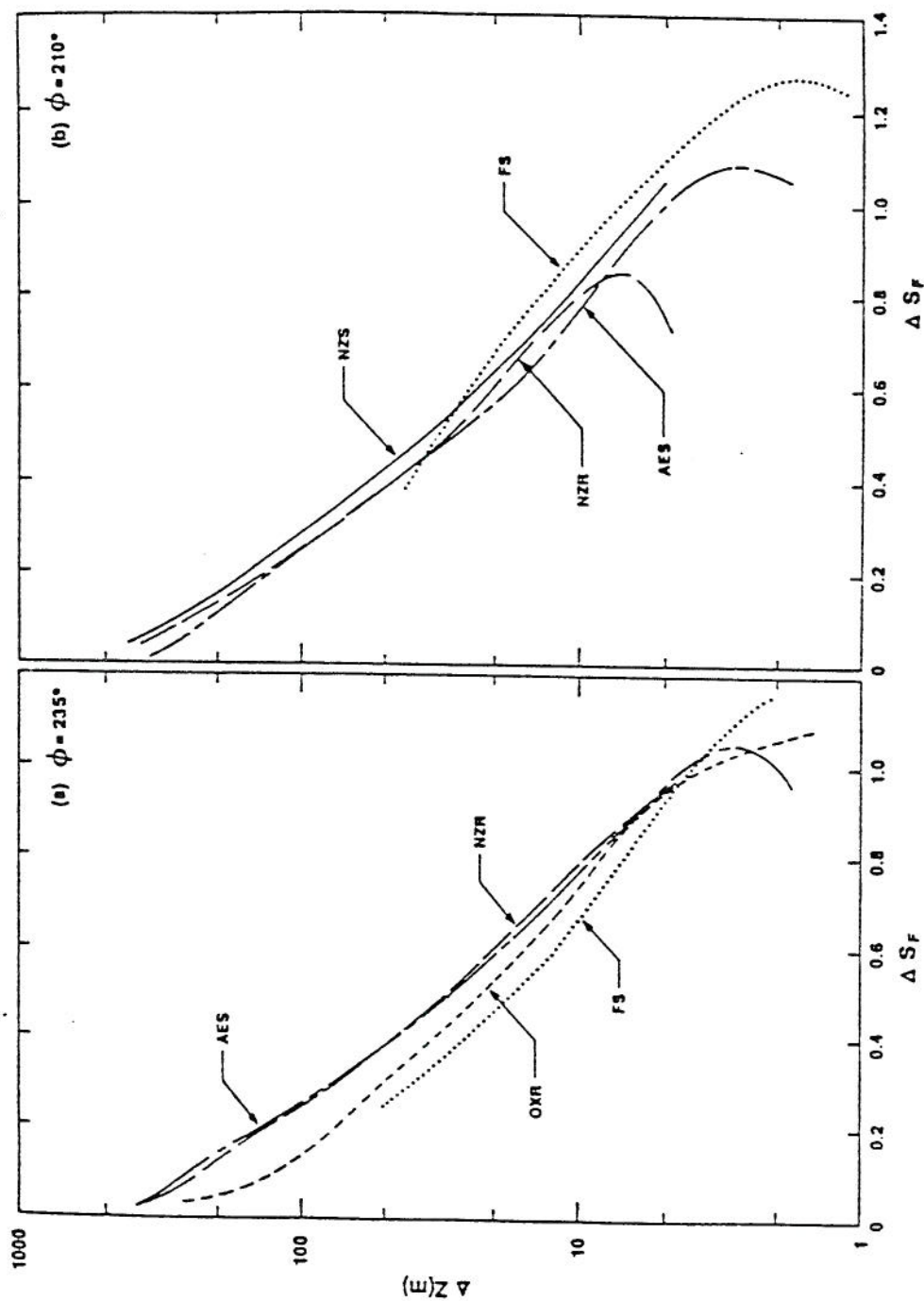


Figure 2.2.1 Vertical profiles of speedup at the hilltop for two wind directions in wind-tunnel (AES, OXR, NZR) and full-scale (FS) flows (Teunissen *et al.*, 1987)

Table 2.2.2.1 Laboratory Simulations of Flow Over Complex Terrain

AUTHOR (DATE)	TOPOGRAPHIC SITE	PROBLEM STUDIED	TYPE OF AIRFLOW	MAXIMUM HEIGHT OF FEATURE (m)	LENGTH SCALE RATIO	deltas/H	alpha	Similarity Criteria $Z_0/H \times 10^{-4}$	u/U_0	L_w/H	RI or PQ Category
*1 Field and Warden (1929-1930)	Rock of Gibraltar	Topographic effects and turbulence	Neutral	520	5000	0.00	0.00				
*2 Abe (1941)	Mt. Fuji, Japan	Mountain clouds and topographic effects	Barostromatic (dry ice)	4000	50000						not accurate
*3 Putnam (1948)	Pond Glastenberg Mt. Washington	Topographic effects	Neutral	300 850 1154	5280 5280 5280		0.00 0.00 0.00				
4 Suzuki & Yabuki (1956)	Idealized hills	Mountain lee waves	Barostromatic (dry ice solution)			0.00	0.00				
5 Long (1953, 1954, 1955)	Idealized hills	Mountain lee waves	Barostromatic (dry ice solution)			0.00	0.00				13-94
* Long (1959)	Sierra Nevada Mtns California	Mountain lee waves	Barostromatic (dry ice solution)	2750	75000	0.00	0.00				12-300
6 Nemoto (1961)	Enoshima & Akashi Channel, Japan	Turbulence & Velocity profiles	Neutral	60	600 3300 10000		1.00	0.20		1.33	
*7 Heltsky, Tolstis, Kepkin & Magony (1962-1963)	Bear Mountain New York	Turbulence & Wake patterns	Neutral	390	1920	1.25		0.16			
8 Briggs (1963)	Rock of Gibraltar	Turbulence Patterns	Neutral	820	5000	0.00	0.00				
9 Heltsky, Magony, & Halpan (1964-65)	Mountains near Manchester, Vermont	Topographic effects	Neutral								
10 Plate & Lin (1965)	Idealized hill	Velocity & turbulence in wake	Neutral Unstable			3-9 3-5	0.16 0.19	1.50 1.50	0.03 0.03		0.02
11 Chang (1966)	Idealized hill	Velocity & turbulence in wake	Neutral			2.00	0.16	1.50			
*12 Cermak, Pateika & Meroney (1966) CSU	Pl. Arguello, CA	Topographic effects Diffusion	Barostromatic Neutral	500 500	12000 12000	9.00 9.00	0.25 0.25				0.31
*13 Meroney & Cermak (1967) CSU	San Nicolas Island, California	Topographic effects Diffusion	Neutral & Barostromatic	275 275	6200 6200	12.60 12.60	0.14 0.20	0.20	0.03		0.30
14 Lin & Binder (1967) CSU	Idealized Mountain	Mountain lee waves	Barostromatic								4-25
15 Garrison & Cermak (1968) CSU	San Bruno Mountain, California	Topographic effects	Neutral Barostromatic (dry ice)	400 400 400	6000/4800 6000/4800 3000/2400	3.70 3.70 1.90	0.16 0.16	25.00 25.00	0.13		0.32 0.32
*16 Hol, Bieder & Cermak (1968) CSU	Green River, Utah	Topographic effects	Neutral	65	800	6.00	0.14	2.00			

Table 2.2.1 (Continued)

AUTHOR (DATE)	TOPOGRAPHIC SITE	PROBLEM STUDIED	TYPE OF AIRFLOW	MAXIMUM HEIGHT OF FEATURE (m)	LENGTH SCALE RATIO	delta/H	alpha	Smakude Criteria $Z/H \times 10^4$	u/H	u/H	L/H	RI or PG Category
17 Sakagami and Kato (1968)	Seashore, Japan	Topographic effects Diffusion	Neutral	500	5000							
18 Zhelevsky, Doroshenko & Chepk (1968)	Idealized Hill	Topographic effects	Neutral									
*19 Lukay (1968)	Fort Mearns West Virginia	Topographic effects Diffusion	Neutral		720							
*20 Kikayashi, Ogil & Carmak (1971) CSU	Elk Mountain, WY	Topographic effects Diffusion	Neutral Barostomatic (Dry Ice)	1200 1200	9600 9600	2.00 2.00	0.21 0.32	70.00		0.16		1.70
*21 Ogil, Carmak & Grant (1971) a CSU	Eagle River Chalk Mountain area Colorado	Topographic effects Diffusion	Neutral Barostomatic (Dry Ice)	1950 1950	9600 9600	4.00 2.00	0.25	3.00	0.28 0.50 0.05 0.60			6.00
*22 Ogil, Carmak & Grant (1971) b CSU	San Juan Mountains Colorado	Topographic effects Diffusion	Neutral Barostomatic	2250 2250	hor 14,000 ver 9,600	2.00 2.00	0.35		0.16 0.20			
*23 Mori, Miyata & Mitsui (1971)	Mt Taketura Japan	Topographical effects	Neutral	300	5000							
24 Maroney, Chaudhry (1971-72) CSU	Rocky Flats Colorado	Topographic effects Diffusion	Neutral	140	1000	3.00	0.14	2.00	0.13			
25 de Bray (1973)	Idealized ramps and escarpments	Speedup	Neutral			3.00 3.00 0.11 0.05	0.14 0.11 0.00		0.12 0.16			
26 Sacre (1973)	Idealized ramps and hills	Speedup	Neutral			3.00	0.15					
27 Counihan (1973)	Idealized ramps and hills		Neutral			8, 12, 20			0.10			
28 Hewson, et al. (1973-75)	Yaquina Head, Oregon	Speedup for WECS	Neutral	15	300	1.70						
29 Freeston (1974)	Idealized hill escarpments	Speedup	Neutral				0.14					
30 Maroney, Carmak (1974-1975) CSU	Mississippi River, Lansing, Iowa	Topographic effects Diffusion	Neutral Barostomatic	150 150	400 400	2.00 2.00	0.27 0.70	60.00 60.00				1.00
*31 Bowen & Lindsay (1974)	Riverbanks and Coastal Beach New Zealand	Speedup	Neutral	10.13	200-250	4.50	0.18	0.60	0.18	0.16		
*32 Lu & Lin (1976)	Idealized Saddle Mountain Garfield, Utah	Topographic effects Diffusion	Barostomatic Barostomatic (brine solution)	1480	10000							0-58 9-35
33 Riley, Lu & Geller (1976)	Idealized hill 3-D	Topographic effects Diffusion	Barostomatic (brine solution)	1480	10000							5-288